

The effect of the neonatal Fc receptor on human IgG biodistribution in mice

Nancy Chen^{1,*}, Weirong Wang¹, Scott Fauty², Yulin Fang¹, Lora Hamuro¹, Azher Hussain¹, and Thomayant Prueksaritanont¹

¹Department of Pharmacokinetics, Pharmacodynamics, and Drug Metabolism; Merck Research Laboratories; West Point, PA USA; ²Department of Laboratory Animal Resources; Merck Research Laboratories; West Point, PA USA

Keywords: FcRn, pharmacokinetics, biodistribution, tissue distribution, monoclonal antibody, IgG,

Abbreviations: pharmacokinetics, PK; intravenous, IV; Trichloroacetic acid, TCA; immunoglobulin G, IgG; neonatal Fc receptor, FcRn; tissue to blood ratio, T/B ratio; area under the curve, AUC; knockout, KO; red blood cell, RBC; Chromium 51, ⁵¹Cr; Iodine 125, ¹²⁵I; wild type, WT; enzyme-linked immunosorbent assay, ELISA

The neonatal Fc receptor (FcRn) plays a pivotal role in IgG homeostasis, i.e., it salvages IgG antibodies from lysosomal degradation following fluid-phase pinocytosis, thus preventing rapid systemic elimination of IgG. Recombinant therapeutic antibodies are typically composed of human or humanized sequences, and their biodistribution, or tissue distribution, is often studied in murine models, although, the effect of FcRn on tissue distribution of human IgG in rodents has not been investigated. In this report, an ¹²⁵I-labeled human IgG1 antibody was studied in both wild type C57BL/6 (WT) and FcRn knockout (KO) mice. Total radioactivity in both plasma and tissues (0–96hr post-dose) was measured by gamma-counting. Plasma exposure of human IgG1 were significantly lower in FcRn KO mice, which is consistent with the primary function of FcRn. Differences in biodistribution of human IgG to selected tissues were also observed. Among the tissue examined, the fat, skin and muscle showed a decrease in tissue-to-blood (T/B) exposure ratio of human IgG1 in FcRn KO mice comparing to the WT mice, while the liver, spleen, kidney, and lung showed an increase in the T/B exposure ratio in FcRn KO mice. A time-dependent change in the T/B ratios of human IgG1 was also observed for many tissues in FcRn KO mice. These results suggest that, in addition to its role in IgG elimination, FcRn may also play a role in antibody biodistribution.

Introduction

Increased understanding of factors that may influence biodistribution could enable the design and development of antibody therapeutic candidates with either increased target tissue localization or decreased off-target tissue distribution, both of which can influence the efficacy or safety of antibody products. However, unlike their small molecule counterparts, factors that can affect the tissue distribution process of therapeutic antibodies are not well-understood.¹ Convection is believed to be the primary mechanism responsible for the transport of antibodies from blood to tissues.² This process depends highly on the vascular permeability, which largely determines the rate of antibody movement from blood to different tissues. For example, the discontinuous capillaries typically found in liver, spleen and bone marrow allow the highest distribution of antibodies to these tissues. In contrast, the capillary endothelium and the underlying basement membrane in the brain are composed of tight junctions, precluding convective distribution of antibodies to the brain.

In addition to variables that affect the processes of both extravasation and interstitial distribution, the neonatal Fc

receptor (FcRn), whose role has been well established in IgG homeostasis,^{3,4} has also been shown to mediate transcytosis of IgG in *in vitro* systems.^{5,6} A previous study by Garg et al. investigated the effect of FcRn in biodistribution via comparison of a murine IgG antibody biodistribution in FcRn knockout (KO) mice and WT mice.⁷ They reported a significant decrease in the tissue-to-blood area under the curve (T/B AUC) ratio in the muscle and skin in FcRn KO mice comparing to WT mice, while the T/B AUC ratio remained similar in other tissues. This suggested that FcRn plays a role in antibody tissue distribution. Garg et al. further proposed that the muscle and skin^{8,9} are among the major sites of IgG catabolism, where FcRn-mediated transport from blood to tissue contributes significantly to IgG extravasation in these two tissues.

FcRn is expressed in many other organs and has been proposed to have additional functions. For example, in the kidney, it had been shown that podocyte FcRn could promote IgG immune complexes clearance through glomerulus, and, at the proximal tubule, FcRn may partly reclaim IgG back into the systemic circulation.¹⁰ FcRn is also expressed at the vascular endothelial cells of the central nervous system (blood-brain barrier).¹¹ There

*Correspondence to: Nancy Chen; Email: nancy.si.chen@gmail.com

Submitted: 10/29/2013; Revised: 01/06/2014; Accepted: 01/08/2014; Published Online: 01/09/2014
<http://dx.doi.org/10.4161/mabs.27765>

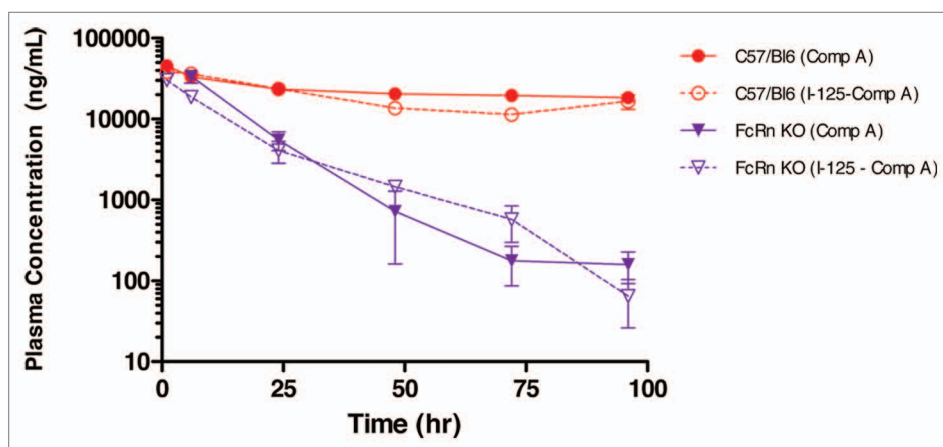


Figure 1. The effect of iodination on plasma pharmacokinetics of Compound A in wild type C57BL/6 (WT) and FcRn knockout (KO) mice, following a 3 mg/kg intravenous bolus administration. Terminal plasma samples were collected for radiolabeled Compound A (dotted line), as measured by gamma counting and each time point is the mean \pm SD ($n = 3$). Serial plasma samples were collected for unlabeled Compound A (solid line), as measured by ELISA, and each data set is mean \pm SD ($n = 3$).

have been controversial reports on whether FcRn behaves as an efflux receptor that can transport antibodies across the blood-brain barrier back into systemic circulation in mouse models.¹²⁻¹⁴

Importantly, interspecies differences in IgG-FcRn interaction have been reported where human IgG binds to mouse FcRn with a higher affinity than human IgG to human FcRn and mouse IgG to mouse FcRn at pH 6.0.¹⁵ It was further shown that the pH 6.0 binding affinity of human IgG1 for mouse FcRn was ~10-fold higher than mouse IgG1 and IgG2b, but comparable to mouse IgG2a.¹⁶ The therapeutic antibodies currently being developed by biopharmaceutical companies are usually human or humanized, and biodistribution is often evaluated in murine models. In this study, we examined the potential effect of FcRn on tissue distribution of a human IgG1 antibody using WT and FcRn KO mouse models. Our results were also compared with the results previously reported by Garg et al., using a murine IgG to examine potential interspecies differences in IgG tissue distribution.

Results

Pharmacokinetics of an ¹²⁵I-labeled human IgG1 molecule (Compound A) in FcRn KO and WT mice

Human IgG1 Compound A, in an unlabeled form, exhibited linear pharmacokinetics in mice, which is typical of a human IgG with no known target in the studied species (data not shown). The pharmacokinetics of ¹²⁵I-labeled Compound A was first characterized in FcRn KO mice and WT mice. Following a single intravenous (IV) dose of 3 mg/kg, the plasma clearance of ¹²⁵I-labeled Compound A in FcRn KO mice was ~8-fold higher than that of WT mice (7.2 ± 0.57 vs 0.91 ± 0.2 mL/hr/kg) (Fig. 1). This is consistent with the known function of FcRn in IgG salvage. The plasma PK profile of ¹²⁵I-labeled Compound A as determined from total radioactivity measurements was compared with that of unlabeled compound as determined by a Compound

A-specific ELISA. The results showed similar plasma PK profiles in both FcRn KO and WT mice (Fig. 1). This suggests that the ¹²⁵I-radiotracer remained associated with systemically circulating Compound A over the 0–96 h time course evaluated, and that radiolabeling did not change the pharmacokinetics behavior of Compound A.

Tissue-to-blood ratios from FcRn KO mice and WT mice

Next, the tissue distribution of Compound A in FcRn KO and WT mice was characterized. Since FcRn is known to affect the clearance of antibodies, the T/B ratio and T/B AUC ratio of Compound A from individual organs was compared between the WT and FcRn KO groups to discern whether FcRn plays any additional

role in tissue distribution.

The tissue radioactivity with or without residue blood correction were evaluated for all tissues. For most of the tissues with relatively high T/B ratio, including skin and muscle, the residue blood correction had very limited effect on the overall tissue radioactivity. Notably, brain was an organ where ¹²⁵I radioactivity from residue blood contributed significantly to the total tissue ¹²⁵I radioactivity. The only other organs where residue blood correction would make a difference were spleen and kidney, but these residue blood corrections would likely lead to deviations from the actual Compound A tissue levels due to the anticipated red blood cell (RBC) turnover in spleen and kidney. Therefore, only tissue ¹²⁵I radioactivity in the brain was reported with residue blood correction, and all other tissue radioactivity was reported without residue blood correction (Fig. 2).

As shown in Figure 2, following a single IV dose of 3 mg/kg Compound A, the organs with more permeable blood capillaries¹⁷ showed higher T/B ratios in both FcRn KO and WT mice. The brain was found to have the lowest T/B ratio, consistent with its least permeable blood capillary. With residue blood correction, the T/B ratio for the brain agreed well with the reported value between 0.1–1% in the literature.^{13,14}

When T/B ratios were compared between FcRn KO and WT mice, the liver and spleen showed a substantially higher T/B ratio in FcRn KO mice than WT mice across the 0–96 h time course (Fig. 2). On the other hand, the fat exhibited lower T/B ratio in FcRn KO mice than WT mice at most of the time points. For most of the other tissues, the T/B ratios were similar between FcRn KO and WT mice at earlier time points, but the ratios increased significantly in FcRn KO mice than WT mice by 96 h (Fig. 2).

To better assess the overall effect of FcRn on tissue distribution, the T/B AUC ratio, i.e., tissue exposure ($\text{Tissue_AUC}_{0-96\text{hr}}$)/blood exposure ($\text{Blood_AUC}_{0-96\text{hr}}$) were compared between FcRn KO and WT mice (Fig. 3). Comparing the T/B AUC ratio

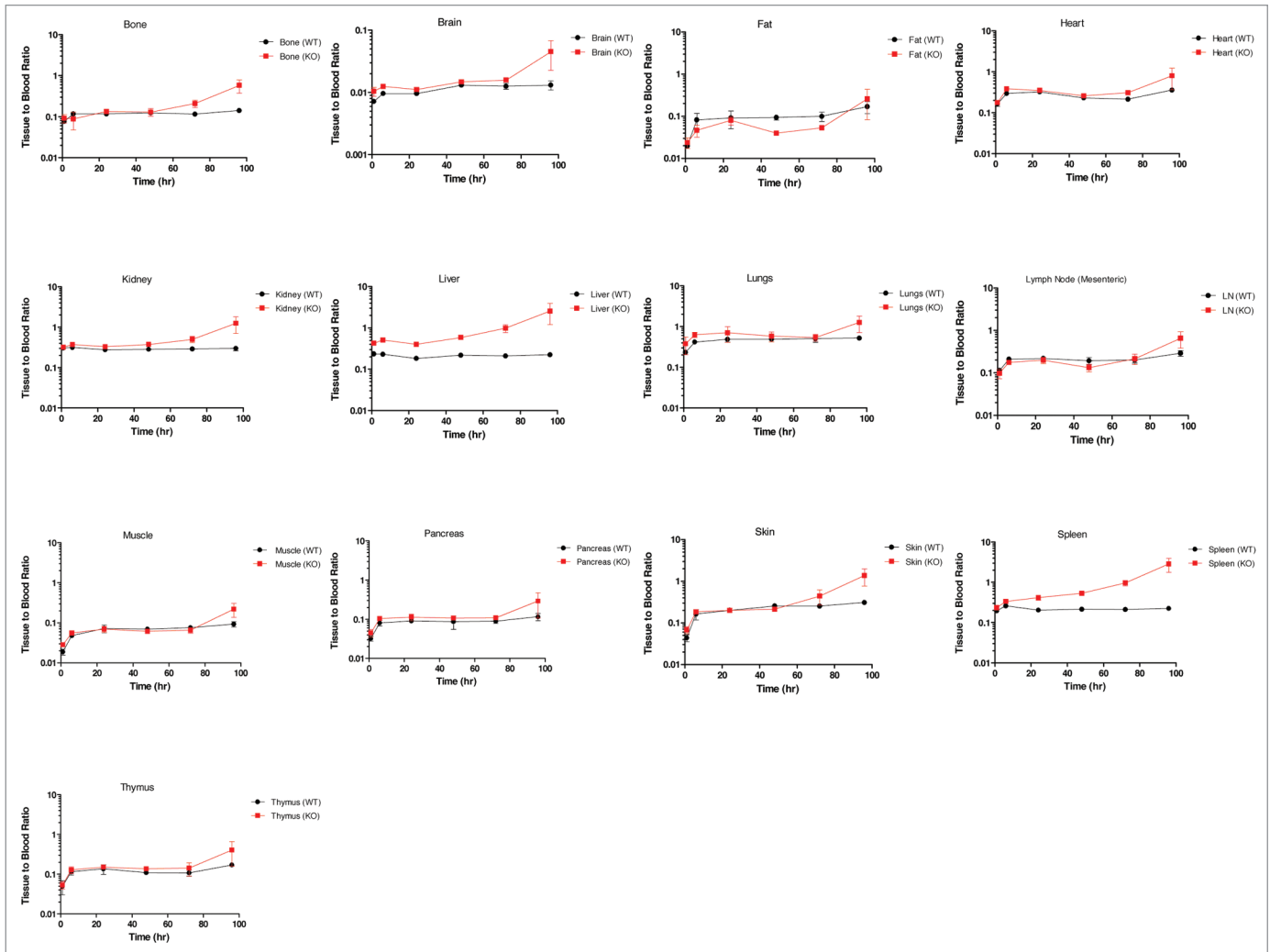


Figure 2. Tissue to blood ratio time course of all collected tissues in wild type (WT) and FcRn knockout (KO) mice. Each time point is a terminal collection of 3 animals from each strain. Each time point is presented as the mean \pm SD.

in FcRn KO mice to that in WT mice, a significant increase was observed in the liver (124%) and spleen (67%), followed by a mild increase in kidney (24%) and lung (30%), a slight decrease in skin (26%), the lymph node (32%), muscle (25%), and the greatest decrease with fat (102%) (Fig. 3).

Analysis of tissue radioactivities

Given the known function of FcRn in IgG salvation, we next examined whether there is any differences in the nature of tissue radioactivity in FcRn KO and WT mice. Trichloroacetic acid (TCA) precipitation was a crude method to assess the nature of observed tissue radioactivity, and it was first conducted with collected liver and kidney samples from both FcRn KO and WT mice. The results showed that the percentage of TCA-precipitable radioactivity from WT mice liver and kidney samples were >90% across all time points. In comparison, the percentage of TCA-precipitable radioactivity from FcRn KO mice tissue samples were >75% across the time course (Fig. 4). The slightly lower % TCA recovery with FcRn KO mice liver and kidney samples were consistent with the anticipated higher IgG catabolism in

FcRn KO mice liver and kidney. But these results suggested it is unlikely that the observed higher T/B ratios in FcRn KO mice can all be attributed to the differences in IgG catabolism. In addition, western blot analysis with polyclonal anti-human Fc antibody was also conducted to look for the presence of breakdown IgG fragments in liver and kidney tissue samples, and no small fragments were detected in either FcRn KO mice or WT mice (data not shown).

Discussion

Our study used a human IgG1 antibody in a murine animal model to further understand the potential role of FcRn in antibody tissue distribution. Given the well-established role of FcRn in IgG homeostasis, we examined the potential role of FcRn in antibody distribution via comparison of the T/B ratio and T/B AUC ratio of a human IgG1 molecule between WT and FcRn KO mice. Compared with WT mice, human IgG1 exhibited different T/B ratios across many organs examined in

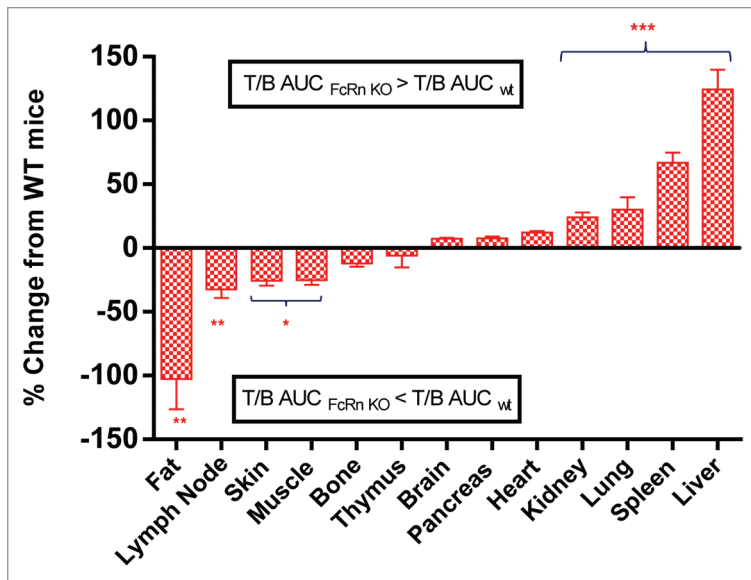


Figure 3. Percentage change of tissue-to-blood area under the curve (T/B AUC) ratio (0–96 h) in FcRn knockout (KO) mice relative to wild-type (WT) mice. The percentage of change was calculated as either an increase or a decrease of $T/B AUC_{KO} / T/B AUC_{WT}$ ratio relative to $T/B AUC_{WT}$. Values are presented as mean \pm s.e.mean. $n = 18$. * $P < 0.05$, ** $P < 0.001$, *** $P < 0.0001$ compared with wild-type mice.

FcRn KO mice. Among them, the liver and spleen exhibited the most significant differences, with the T/B AUC ratios in FcRn KO mice being $124 \pm 15.3\%$ and $67 \pm 8.2\%$ higher than that in WT mice, respectively. The increase of T/B ratio of IgG1 in the liver and spleen appeared to increase with time. In fact, an apparent higher T/B ratio of IgG1 at 96hr was observed in many other organs. On the other hand, T/B AUC ratios showed a mild to moderate decrease in the skin, muscle and fat in FcRn KO mice compared with that in WT mice. Together the results suggested that FcRn may have a broad effect on tissue selectivity of IgG.

The role of FcRn in protection of IgG from intracellular catabolism indeed could have affected tissue distribution of human IgG, considering the significant higher systemic clearance of IgG in FcRn KO mice and relatively slow elimination of IgG from the tissues. We analyzed the liver and kidneys samples from both FcRn KO mice and WT mice with TCA precipitation and western blot. Despite the caveats of both technologies, the results from both experiments suggested that catabolism was not likely a major contributing factor for the observed differences in T/B ratio between FcRn KO and WT mice. Based on our current results, and the observed various tissue distribution pattern changes in FcRn KO mice, we believe it is more likely that FcRn also play roles in transporting antibody into, or out of, specific organs. This is consistent with the reported widespread expression of FcRn in tissues, including the liver,¹⁸ bone marrow,^{19,20} lungs,²¹ kidneys,^{10,22} skin,^{23,24} and spleen.²⁵ For example, the T/B ratios of IgG1 in the liver and spleen were higher in FcRn KO mice across all time points. FcRn in the liver or spleen may serve as a transcytosis mechanism that transports the IgG out of the tissue.

It was previously shown that many types of cells within the liver and spleen express FcRn, e.g., hepatocytes, Kupffer cells, sinusoidal endothelial cells,^{18,26} and monocytes, macrophages, and lymphocytes.^{20,28} The extent of recycling and transcytosis by FcRn may vary within each of these cell types. Tzaban et al. demonstrated that, in polarized epithelial cells, FcRn traffics IgG from either apical or basolateral membranes into the recycling endosome, where it is a critical sorting station, distinguishing between the recycling and transcytotic pathways.²⁷ The T/B ratios of IgG1 in the kidney were similar between FcRn KO mice and WT mice at earlier time points, but were much higher at 72 and 96 h in FcRn KO mice than that in WT mice. It had been suggested that FcRn expressed in the kidney serves in immune surveillance, preventing the accumulation of IgG immune complexes during the filtration process.^{22,29} It was demonstrated previously in FcRn KO mice that FcRn in the podocytes promote IgG clearance and the ones in the proximal tubule epithelial cells reclaim IgG back into the systemic circulation.³⁰ Our data supports the potential IgG secretion role of FcRn in the kidney.

Our data are consistent with the previous report that showed skin and muscles exhibited lower T/B AUC ratio in FcRn KO mice,⁷ which suggests that FcRn may play a role in transporting IgGs from blood circulation to these tissues. The differences we observed were to a less extent, i.e., $\sim 25\%$ vs. $\sim 53\%$, comparing to the findings from Garg et al. A more pronounced decrease in T/B AUC ratio was found with fat in our study, and it was not studied by Garg et al. Similar to what was reported by Garg et al.¹³ and Abuqayyas and Balthasar,¹⁴ we showed there was no T/B AUC ratio difference between FcRn KO mice and WT mice in the brain, and no T/B ratio difference except the last time point (96 h), which suggested that FcRn has little effect on distribution of IgG in the brain.

Notably, we found tissue selectivity of IgG biodistribution in the liver, spleen and kidney, which was not found by Garg et al. One possible explanation could be the use of the α chain FcRn KO mouse model in our study compared with the $\beta 2$ -microglobulin FcRn KO mouse model used by Garg et al. The α chain KO model is more specific to FcRn; $\beta 2$ -microglobulin is a component of all MHC class I molecule and knocking out $\beta 2$ -microglobulin may affect the function of other proteins.³¹ Another important difference is that human IgG was used in the current study whereas Garg et al. used a murine IgG antibody. Based on our in-house data and data in the literature, differences up to 10-fold in FcRn binding affinity across species were observed.¹⁵ The potential inter-species differences in the role of FcRn in IgG biodistribution clearly warrant more studies in the future.

In summary, FcRn KO mice exhibit notable changes in human IgG biodistribution compared with WT mice, and the direction and extent of the effect varies from organ to organ. These results suggested a possible role of FcRn in IgG biodistribution, in addition to its well-established role in protecting IgG from intracellular catabolism.

Materials and Methods

Radiolabeling of Compound A with Iodine-125 (^{125}I) for tissue distribution

Compound A is a human IgG1 monoclonal antibody developed in-house by Merck and Co. It has no known biological binding target in mice. It binds to both human and murine FcRn receptor with ~ 10 -fold higher affinity than that of murine IgG1 antibody (data not shown). Compound A was labeled with ^{125}I NaI (Perkin Elmer) using modified Pierce Iodobeads iodination method (Thermo Scientific). Briefly, 100 μg of protein dialyzed into phosphate buffered saline was incubated with 1 mCi of Iodine-125 (^{125}I) (Perkin Elmer) and two Iodobeads for 15 min at room temperature. The labeled protein was purified with a Zeba column (Pierce), and stored at 4 $^{\circ}\text{C}$. The radiochemical concentration was determined by gamma counting using Wallac 1470 automated gamma counter (Perkin Elmer). The purity of labeled proteins was determined by size-exclusion high-performance liquid chromatography with a gamma detector. The percentage of free ^{125}I was less than 2% in all preparations. The integrity of labeled proteins was also analyzed with a product-specific immunoassay (Quantikine IVD human erythropoietin kits, R&D System) and the labeled Compound A showed comparable concentration-response curves to corresponding unlabeled materials.

Radiolabeling of RBCs with chromium-51 (^{51}Cr)

To determine the contribution of residual blood in overall tissue radioactivity, ^{51}Cr -labeled RBCs were prepared and co-injected with ^{125}I -labeled Compound A. The RBC labeling procedure was modified from the method proposed by the International Committee for Standardization in Hematology (ICSH, 1973).³² Briefly, about 2.5 mL of fresh sterile blood was collected in EDTA tubes from untreated C57BL/6 mice. Blood was centrifuged at 1500 rpm for 5 min at room temperature. The supernatant was discarded and the pellet was washed three times with sterile isotonic sodium chloride. The cell pellet was reconstituted with 0.5 mL of sterile saline. One millicurie of $\text{Na}_2^{51}\text{CrO}_4$ was added to the newly reconstituted cell suspension. The mixture was incubated for 45 min at room temperature with intermittent gentle pipetting. The supernatant was removed after the cell suspension was centrifuged at 1500 rpm for 5 min. The pellet was washed 4–5 times ($5 \times$ volume of RBCs) with sterile saline until most of the free ^{51}Cr was removed ($\sim 0.01\%$ of total radiolabeled RBC activity). Lastly the pellet was reconstituted with desired volume of sterile saline to achieved required concentration of ^{51}Cr -labeled RBCs.

Pharmacokinetics study of ^{125}I -labeled and unlabeled Compound A in FcRn KO and C57BL/6 mice

There were two strains of mice used in our studies: B6.129X1-Fcgrt^{tm1Dcr/DcrJ}, the homozygous FcRn α -chain knockout mice (KO), and C57BL/6 wild type mice (WT), the parental strain of the FcRn KO mice. Both strains were obtained from The Jackson

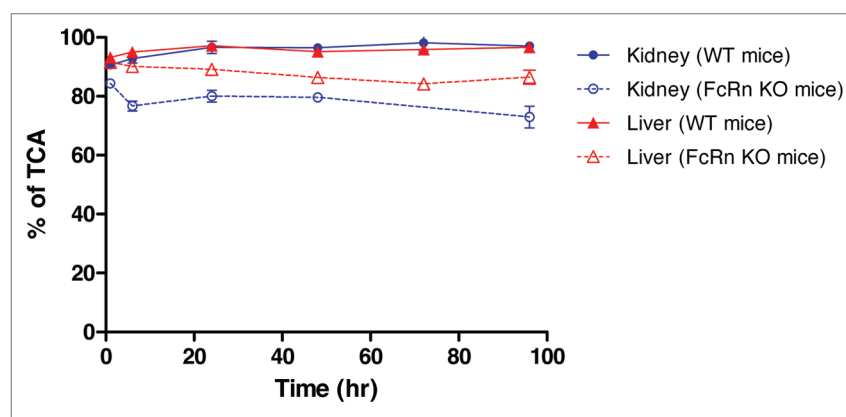


Figure 4. Percentage of post-TCA precipitation of the kidney and liver samples in C57BL/6 wild-type (WT) and FcRn knockout (KO) mice. Each time point is a terminal collection of 3 animals from each strain. Each time point is presented as the mean \pm SD.

Laboratory (Bar Harbor, ME). All animal studies were approved by, and conducted according to, the Merck Institutional Animal Care and Use Committee.

Two days before the experiment, mice were given Lugol's solution (potassium iodide) in drinking water to block excess uptake of free iodide into thyroid. ^{125}I -labeled Compound A, at a dose of 3 mg/kg (400 $\mu\text{Ci}/\text{kg}$ ^{125}I activity, ~ 8 μCi per mouse), was mixed with 600 $\mu\text{Ci}/\text{kg}$ of ^{51}Cr -labeled RBCs (~ 12 μCi per mouse). The mixture was dosed intravenously (IV) via the tail vein to the FcRn KO and C57BL/6 WT mice, respectively. At various time points (i.e., 1, 6, 24, 48, 72, and 96 h), three animals from each group at each time point were sacrificed. Blood, bone, brain, fat, heart, kidney, liver, lung, lymph node (mesenteric), muscle, pancreas, skin, spleen, stomach and thymus were collected and weighed in polypropylene tubes. ^{125}I and ^{51}Cr activities were measured by Wizard 1470 automated gamma counter (Perkin Elmer). Radioactivity was corrected for background and decay. Total tissue radioactivity with and without residual blood correction were measured for all tissues collected. The amount of residual blood in a tissue was calculated from the ^{51}Cr activity in tissue over ^{51}Cr activity in blood, which in turn was used to correct tissue Compound A radioactivity (total ^{125}I radioactivity - ^{125}I radioactivity from residue blood).

The plasma concentrations of unlabeled Compound A were determined by an enzyme-linked immunosorbent assay (ELISA). In brief, a biotinylated mouse anti-human κ chain monoclonal antibody (BD PharMingen) was used for capture, and a mouse anti-human IgG (Fc)-conjugated with HRP was used for detection. The antibody concentration was extrapolated from the standard curve with the lower limit of quantitation of 100 ng/mL. Standard non-compartmental analyses were performed to determine the clearance and AUC of labeled and unlabeled Compound A using WinNonlin (Enterprise Version 5.2.1, Pharsight Corp).

Tissue sample analysis

Each tissue was previously weighed and its radioactive concentration was determined by using a Wallac 1470 automated gamma counter (Perkin Elmer). Protein dilution

factor, radioisotope decay factor and specific activity were taken into account for drug concentration calculation in each tissue. TCA precipitation of tissue homogenate was performed after homogenizing the kidney and liver.³³ The tissue homogenate was centrifuged at 5000 rpm for 20 min at 4 °C and the supernatant was collected. Two hundred μ L of the collected matrix was added to 200 μ L of 10% ice cold TCA. The samples were shaken at 1200 rpm for 10 min at 4 °C and then centrifuged at 14000 rcf for 5 min at 4 °C. The supernatant was aspirated and the TCA-precipitable radioactivity in the pellet was measured by the gamma counter. Tissue drug levels were calculated from post-TCA radioactivity and the specific activity of dosing solutions with the correction of ¹²⁵I decay (ng-eq/ml). The %TCA of a sample was calculated as post-TCA/pre-TCA (%), which is an indication of the integrity of the labeled protein, i.e., the % of radioactivity that remains protein-associated. The AUC of tissue-to-blood (T/B) ratios over the 0–96 h period were compared

between WT and FcRn KO mice to evaluate the effect of FcRn on tissue distribution of human IgG1. The variance of AUC ratio was calculated using the formula of propagation of error:³⁴ $SE_{\text{ratio}} = \text{AUC}_{\text{ratio}} (T/B) * \text{Square Root} [(\text{SEM}_{\text{tissue}}/\text{AUC}_{\text{tissue}})^2 + (\text{SEM}_{\text{blood}}/\text{AUC}_{\text{blood}})^2]$. Tissue-to-blood AUC ratios between WT and FcRn KO mice were compared by using one-way ANOVA test. Analysis was performed using GraphPad InStat 6.0.

Disclosure of Potential Conflicts of Interest

Chen N, Wang W, Fauty S, Fang Y, Hamuro L, Hussain A, and Prueksaritanont T are employees of Merck Research Laboratories, which supported the study financially.

Acknowledgments

We would like to thank Ken Koeplinger and Brian Carr for their insightful comments and helpful suggestions for the manuscript.

References

1. Prueksaritanont T, Tang C. ADME of biologics—what have we learned from small molecules? *AAPS J* 2012; 14:410-9; PMID:22484625; <http://dx.doi.org/10.1208/s12248-012-9353-6>
2. Wang W, Wang EQ, Balthasar JP. Monoclonal antibody pharmacokinetics and pharmacodynamics. *Clin Pharmacol Ther* 2008; 84:548-58; PMID:18784655; <http://dx.doi.org/10.1038/clpt.2008.170>
3. Brambell FW. The transmission of immunity from mother to young and the catabolism of immunoglobulins. *Lancet* 1966; 2:1087-93; PMID:4162525; [http://dx.doi.org/10.1016/S0140-6736\(66\)92190-8](http://dx.doi.org/10.1016/S0140-6736(66)92190-8)
4. Ghetie V, Ward ES. FcRn: the MHC class I-related receptor that is more than an IgG transporter. *Immunol Today* 1997; 18:592-8; PMID:9425738; [http://dx.doi.org/10.1016/S0167-5699\(97\)01172-9](http://dx.doi.org/10.1016/S0167-5699(97)01172-9)
5. Praetor A, Ellinger I, Hunziker W. Intracellular traffic of the MHC class I-like IgG Fc receptor, FcRn, expressed in epithelial MDCK cells. *J Cell Sci* 1999; 112:2291-9; PMID:10381385
6. McCarthy KM, Yoong Y, Simister NE. Bidirectional transcytosis of IgG by the rat neonatal Fc receptor expressed in a rat kidney cell line: a system to study protein transport across epithelia. *J Cell Sci* 2000; 113:1277-85; PMID:10704378
7. Garg A, Balthasar JP. Physiologically-based pharmacokinetic (PBPK) model to predict IgG tissue kinetics in wild-type and FcRn-knockout mice. *J Pharmacokinetic Pharmacodyn* 2007; 34:687-709; PMID:17636457; <http://dx.doi.org/10.1007/s10928-007-9065-1>
8. Deng R, Meng YG, Hoyte K, Lutman J, Lu Y, Iyer S, DeForge LE, Theil FP, Fielder PJ, Prabhu S. Subcutaneous bioavailability of therapeutic antibodies as a function of FcRn binding affinity in mice. *MAbs* 2012; 4:101-9; PMID:22327433; <http://dx.doi.org/10.4161/mabs.4.1.18543>
9. Kagan L, Mager DE. Mechanisms of subcutaneous absorption of rituximab in rats. *Drug Metab Dispos* 2013; 41:248-55; PMID:23129212; <http://dx.doi.org/10.1124/dmd.112.048496>
10. Kobayashi N, Suzuki Y, Tsuge T, Okumura K, Ra C, Tomino Y. FcRn-mediated transcytosis of immunoglobulin G in human renal proximal tubular epithelial cells. *Am J Physiol Renal Physiol* 2002; 282:F358-65; PMID:11788451
11. Schlachetzki F, Zhu C, Pardridge WM. Expression of the neonatal Fc receptor (FcRn) at the blood-brain barrier. *J Neurochem* 2002; 81:203-6; PMID:12067234; <http://dx.doi.org/10.1046/j.1471-4159.2002.00840.x>
12. Deane R, Sagare A, Hamm K, Parisi M, LaRue B, Guo H, Wu Z, Holtzman DM, Zlokovic BV. IgG-assisted age-dependent clearance of Alzheimer's amyloid beta peptide by the blood-brain barrier neonatal Fc receptor. *J Neurosci* 2005; 25:11495-503; PMID:16354907; <http://dx.doi.org/10.1523/JNEUROSCI.3697-05.2005>
13. Garg A, Balthasar JP. Investigation of the influence of FcRn on the distribution of IgG to the brain. *AAPS J* 2009; 11:553-7; PMID:19636712; <http://dx.doi.org/10.1208/s12248-009-9129-9>
14. Abuqayyas L, Balthasar JP. Investigation of the role of FcγR and FcRn in mAb distribution to the brain. *Mol Pharm* 2013; 10:1505-13; PMID:22838637; <http://dx.doi.org/10.1021/mp300214k>
15. Ober RJ, Radu CG, Ghetie V, Ward ES. Differences in promiscuity for antibody-FcRn interactions across species: implications for therapeutic antibodies. *Int Immunol* 2001; 13:1551-9; PMID:11717196; <http://dx.doi.org/10.1093/intimm/13.12.1551>
16. Zhou J, Johnson JE, Ghetie V, Ober RJ, Ward ES. Generation of mutated variants of the human form of the MHC class I-related receptor, FcRn, with increased affinity for mouse immunoglobulin G. *J Mol Biol* 2003; 332:901-13; PMID:12972260; [http://dx.doi.org/10.1016/S0022-2836\(03\)00952-5](http://dx.doi.org/10.1016/S0022-2836(03)00952-5)
17. Zweifach BW. Permeability aspects of blood tissue exchange. *Invest Ophthalmol* 1965; 4:1065-74; PMID:5321924
18. Blumberg RS, Koss T, Story CM, Barisani D, Polischuk J, Lipin A, Pablo L, Green R, Simister NE. A major histocompatibility complex class I-related Fc receptor for IgG on rat hepatocytes. *J Clin Invest* 1995; 95:2397-402; PMID:7738203; <http://dx.doi.org/10.1172/JCI117934>
19. Akilesh S, Christianson GJ, Roopenian DC, Shaw AS. Neonatal FcR expression in bone marrow-derived cells functions to protect serum IgG from catabolism. *J Immunol* 2007; 179:4580-8; PMID:17878355
20. Montoyo HP, Vaccaro C, Hafner M, Ober RJ, Mueller W, Ward ES. Conditional deletion of the MHC class I-related receptor FcRn reveals the sites of IgG homeostasis in mice. *Proc Natl Acad Sci U S A* 2009; 106:2788-93; PMID:19188594; <http://dx.doi.org/10.1073/pnas.0810796106>
21. Spiekermann GM, Finn PW, Ward ES, Dumont J, Dickinson BL, Blumberg RS, Lencer WI. Receptor-mediated immunoglobulin G transport across mucosal barriers in adult life: functional expression of FcRn in the mammalian lung. *J Exp Med* 2002; 196:303-10; PMID:12163559; <http://dx.doi.org/10.1084/jem.20020400>
22. Haymann JP, Levraud JP, Bouet S, Kappes V, Hagege J, Nguyen G, Xu Y, Rondeau E, Sraer JD. Characterization and localization of the neonatal Fc receptor in adult human kidney. *J Am Soc Nephrol* 2000; 11:632-9; PMID:10752522
23. Cauza K, Hinterhuber G, Dingelmaier-Hovorka R, Brugger K, Klosner G, Horvat R, Wolff K, Foedinger D. Expression of FcRn, the MHC class I-related receptor for IgG, in human keratinocytes. *J Invest Dermatol* 2005; 124:132-9; PMID:15654966; <http://dx.doi.org/10.1111/j.0022-202X.2004.23542.x>
24. Cianga P, Cianga C, Plamadeala P, Branisteanu D, Carasevici E. The neonatal Fc receptor (FcRn) expression in the human skin. *Virchows Arch* 2007; 451:859-60; PMID:17674040; <http://dx.doi.org/10.1007/s00428-007-0467-7>
25. Ghetie V, Hubbard JG, Kim JK, Tsen MF, Lee Y, Ward ES. Abnormally short serum half-lives of IgG in beta 2-microglobulin-deficient mice. *Eur J Immunol* 1996; 26:690-6; PMID:8605939; <http://dx.doi.org/10.1002/eji.1830260327>
26. Cianga C, Cianga P, Plamadeala P, Amalinei C. Nonclassical major histocompatibility complex I-like Fc neonatal receptor (FcRn) expression in neonatal human tissues. *Hum Immunol* 2011; 72:1176-87; PMID:21978715; <http://dx.doi.org/10.1016/j.humimm.2011.08.020>
27. Tzaban S, Massol RH, Yen E, Hamman W, Frank SR, Lapierre LA, Hansen SH, Goldenring JR, Blumberg RS, Lencer WI. The recycling and transcytotic pathways for IgG transport by FcRn are distinct and display an inherent polarity. *J Cell Biol* 2009; 185:673-84; PMID:19451275; <http://dx.doi.org/10.1083/jcb.200809122>
28. Antohe F, Radulescu L, Gafencu A, Ghetie V, Simionescu M. Expression of functionally active FcRn and the differentiated bidirectional transport of IgG in human placental endothelial cells. *Hum Immunol* 2001; 62:93-105; PMID:11182218; [http://dx.doi.org/10.1016/S0198-8859\(00\)00244-5](http://dx.doi.org/10.1016/S0198-8859(00)00244-5)
29. Akilesh S, Huber TB, Wu H, Wang G, Hartleben B, Kopp JB, Miner JH, Roopenian DC, Unanue ER, Shaw AS. Podocytes use FcRn to clear IgG from the glomerular basement membrane. *Proc Natl Acad Sci U S A* 2008; 105:967-72; PMID:18198272; <http://dx.doi.org/10.1073/pnas.0711515105>

30. Sarav M, Wang Y, Hack BK, Chang A, Jensen M, Bao L, Quigg RJ. Renal FcRn reclaims albumin but facilitates elimination of IgG. *J Am Soc Nephrol* 2009; 20:1941-52; PMID:19661163; <http://dx.doi.org/10.1681/ASN.2008090976>
31. Simister NE, Mostov KE. An Fc receptor structurally related to MHC class I antigens. *Nature* 1989; 337:184-7; PMID:2911353; <http://dx.doi.org/10.1038/337184a0>
32. International Committee for Standardization in Hematology (ICSH) Panel on Diagnostic Applications of Radioisotopes in Haematology. Standard techniques for the measurement of red-cell and plasma volume. *Br J Haematol* 1973; 25:801-14; PMID:4586522; <http://dx.doi.org/10.1111/j.1365-2141.1973.tb01792.x>
33. Bensadoun A, Weinstein D. Assay of proteins in the presence of interfering materials. *Anal Biochem* 1976; 70:241-50; PMID:1259145; [http://dx.doi.org/10.1016/S0003-2697\(76\)80064-4](http://dx.doi.org/10.1016/S0003-2697(76)80064-4)
34. Motulsky H. *Intuitive biostatistics*. 1995. Oxford University Press, New York.